Joint Special Interest Group meeting between euspen and ASPE
Dimensional Accuracy and Surface Finish in Additive Manufacturing,
KU Leuven, BE, October 2017
www.euspen.eu

CT dimensional evaluations of 3D cellular structures produced by selective laser melting

E. Sbettega[1], F. Zanini[1], M. Benedetti[2], E. Savio[3], S. Carmignato[1]

[1]*Department of Management and Engineering, University of Padua, Vicenza, Italy.*
[2]*Department of Industrial Engineering, University of Trento, Trento, Italy.*
[3]*Department of Industrial Engineering, University of Padua, Padua, Italy.*

filippo.zanini@unipd.it

Abstract
The use of Additive Manufacturing (AM) technologies is rapidly expanding in biomedical engineering, e.g. in connection with replacement and stabilization of damaged bone tissues. Selective laser melting (SLM) allows producing titanium structures that can be adjusted to bone tissue characteristics and overcome limitations of traditional manufacturing. Since SLM products can be characterized by significant geometrical and surface deviations, appropriate quality control methods are required. In this work, Ti6Al4V cellular structures produced by SLM with different periodic lattice designs were analysed using a metrological X-ray computed tomography (CT) system, to characterise their geometry, thickness distribution and surface morphology. Moreover, specific investigations were performed to understand the accuracy of CT dimensional measurements of SLM cellular structures.

1. Introduction

The use of metal AM technologies is constantly expanding in several industrial sectors, especially for the production of components having complex geometry and high structural complexity [1]. In particular, selective laser melting is capable of fabricating strong and complex metallic lattice structures [2], which are impossible to be obtained through conventional manufacturing techniques (e.g. machining and casting) [3]. The production of such lattice structures is relevant in biomedical engineering. For example, when the replacement and stabilization of damaged bone tissues is performed using fully dense titanium alloy implants, the resulting stiffness is higher than that of the bone tissue. To avoid the consequent stress-shielding, the most used approach is to reduce the implant stiffness [4]. AM controlled cellular structures allows a better adjustment to bone tissues, overcoming the abovementioned issue. However, significant differences between designed and as-produced parts can be obtained [5]. In fact, AM products are inherently characterized by poor geometrical accuracy and complex surface morphology, which can lead to mechanical properties degradation and product failure. In order to verify the quality of AM lattice structures and to optimize the AM process, accurate geometrical and morphological measurements are needed. Micro X-ray computed tomography (CT) is an advanced measuring technique that can be effectively used for AM components [6, 7], including cellular specimens [8], as it is capable of examining non-destructively features and structures that are inaccessible with other measuring techniques. Examples of CT evaluations that can be performed on cellular components are CAD comparison and thickness analysis [5]. Investigations performed in this work were focused on studying challenges and accuracy of such dimensional analyses on SLM cellular structures.

2. Components and instrumentation

2.1. SLM cellular specimens

In this work, six cellular specimens (named with letters from A to F) produced by SLM of Ti-6Al-4V alloy were investigated (see Figure 1). These specimens are characterized by specific lattice designs, i.e. periodic structures determined by square cells packed in six different ways in 3D space. The different structures were designed using Finite Elements method (FEM) to obtain an elastic modulus of roughly 3 GPa in order to match that of trabecular bone.

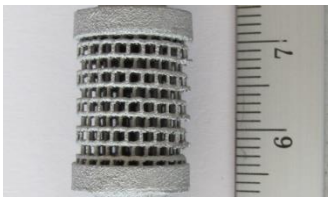

Figure 1. Example of SLM cellular specimen made of Ti6Al4V.

2.2. CT scanning

The cellular specimens described in Section 2.1 were scanned by a metrological CT system (Nikon Metrology MCT225) characterized by micro-focus X-ray tube, 16 bit detector with 2000×2000 pixels, high-precision linear guideways and thermally controlled cabinet. The scanning parameters reported in Table 1 were applied for all the specimens.

Table 1 CT scanning parameters.

Parameter	Value
Voltage	180 kV
Current	38 µA
Exposure time	2000 ms
Nr. of projections	3142
Voxel size	8.3 µm

3. Description of CT-based analyses

3.1. CAD comparison

Each specimen was produced by SLM, starting from computer-aided design (CAD) data. The same CAD models used for production were used also as nominal geometry to be compared with the CT-measured geometry. The comparison was performed using the software VGStudio MAX 3.0 (Volume Graphics GmbH, Germany) after aligning the actual volume with the nominal model by means of Gaussian best-fit. The outcome of the comparison is a color-coded map of deviations (expressed in millimetres), as shown in Figure 2.

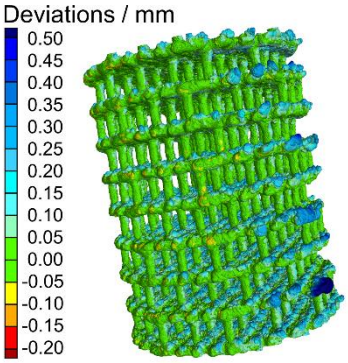

Figure 2. Color-coded map of deviations between CT-measured part (specimen A) and nominal model.

3.2. Structural distortions

Cellular structures produced by additive manufacturing can present significant structural distortions [9]. In this work, a new Matlab (MathWorks, USA) routine was implemented to identify the spatial coordinates of nodes using a point cloud extracted from the CT scanned volumes. The actual position of nodes was then compared with their nominal position.

3.3. Thickness analysis

The thickness distribution of the cellular structures was evaluated using a dedicated module of VGStudio MAX 3.0 and was then compared with the nominal thickness. Such analysis does not require an alignment between measured geometry and nominal model. The main parameter to be defined is the search angle, centred on the lines perpendicular to the two opposite surfaces considered for the starting point and the end point.

3.4. Evaluation of surface topography

CT has been recently utilized for topography evaluations of AM surfaces [10], including surfaces not accessible by other instruments. The evaluation of surface roughness is relevant as it is connected to the process quality and also because it can influence the dimensional measurements performed by CT [11]. In this work, the surface of cellular specimens was analysed on areas randomly selected inside the part on nominally cylindrical portions after the subtraction of a least-squares mean cylinder (surface S-F), in terms of *Sa* and *Sz* parameters [12].

4. Results and discussions

Results obtained from the comparison between each CT-measured part and the corresponding nominal model are reported in Figure 3, which illustrates the amount of surface area (normalized against the total surface area) interested by each specific deviation. As shown in Fig. 3, the measured deviations are mainly positive for each specimen.

The structural analysis (see Section 3.2) revealed that significant structural distortions characterize the as-produced specimens, as depicted in Figure 4.

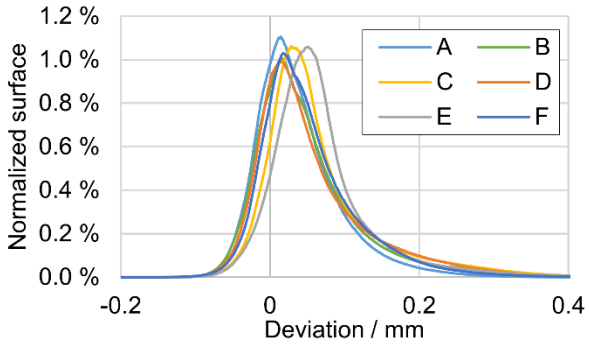

Figure 3. Distribution of deviations between CT-measured part and nominal model.

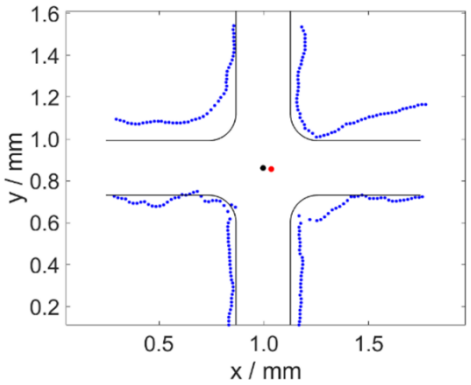

Figure 4. Real node (red point, obtained by CT data) compared with the corresponding nominal node (black point) of specimen C. Black lines represent the CAD model and blue dots represent the measured surface.

The deviations determined form the CAD comparison include both geometrical/dimensional errors and structural errors. For this reason, when the interest is on evaluating only the errors associated with the local dimensions, a thickness analysis is more effective. A first thickness analysis was conducted using the default value proposed by the software for the search angle (i.e. 30°; see Section 3.3). A peak of very low thickness was found for each specimen, as visible in Figure 5 where specimens B, D and E are taken as examples. Table 2 lists the total surface area obtained with search angle 30° (named S_{30}) related to thickness values ranging from 0 to 0.07 mm calculated from diagrams as those reported in Figure 5. The presence of these peaks was observed to be related to the complex topography of the surface with high form errors and high surface roughness, as shown in Figure 6 (where the surface of specimens B and E are compared). Sample B has a higher roughness than sample E, confirmed by *Sa* and *Sz* parameters, which are 27 and 267 µm respectively for sample B, and 19 and 157 µm for sample E.

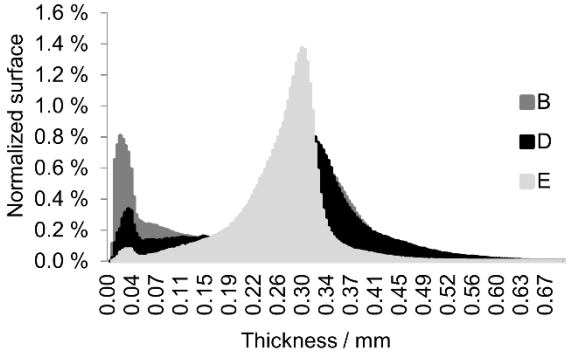

Figure 5. (a) Thickness distribution for samples B, D and E (thickness analysis performed with search angle 30°).

Table 2 Total surface area related to thickness values ranging from 0 to 0.07 mm obtained with search angles of 30° (S_{30}) and 15° (S_{15}).

	A	B	C	D	E	F
S_{30} / mm²	108.0	362.3	19.3	73.7	14.2	105.5
S_{15} / mm²	36.4	114.1	6.0	23.2	4.2	34.5

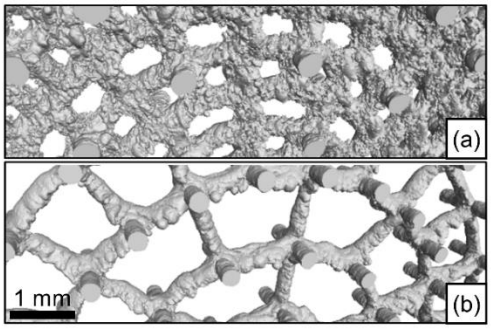

Figure 6. Regions of interest of sample B (a) and sample E (b); different surface topographies can be observed for the two different samples.

The combined influence of the surface topography and the search angle on the thickness analysis was analysed by simulating five cylindrical features with different surface topography and known thickness distribution (see Figure 7).

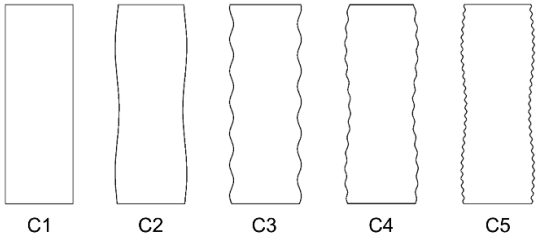

Figure 7. Cylindrical features with height equal to 1 mm, obtained from the 360°-rotation of different sinusoidal functions (C1: $y = 0.17$; C2: $y = 0.17 + (\sin 10x/100)$; C3: $y = 0.17 + (\sin 40x/100)$; C4: $y = 0.17 + (\sin 10x/100) + (\sin 80x/200)$; C5: $y = 0.17 + (\sin 10x/100) + (\sin 160x/200)$) around the central axis.

Figure 8 reports the percentage deviations obtained by comparing the measured mean thickness (weighted on the surface area interested by each thickness) with its corresponding reference value. The error related to the mapped surface (i.e. the surface actually analysed by the algorithm) is reported as well. The search angle 15° was determined to allow mapping well the surface while keeping deviations under 5%.

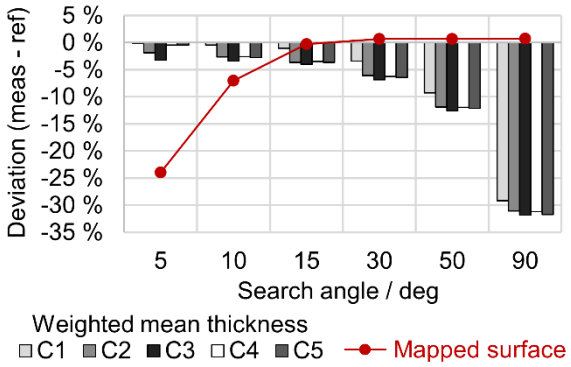

Figure 8. Relative deviations (measured - reference) of the five simulated cylindrical features, concerning the mean thickness (weighted on the surface interested by each thickness) and the mapped surface, for different search angles.

The thickness analysis was performed again on the SLM specimens by setting the search angle to 15° and the surface area S_{15} was observed to decrease systematically by 70% with respect to S_{30} (see Table 2). The same cylindrical features were used to investigate the influence of different surface topographies on the CAD comparison analysis. Table 3 shows that the CAD comparison analysis leads to small errors concerning each simulated cylindrical feature.

Table 3 Percentage errors resulting from CAD comparison performed on five simulated cylindrical features with varying surface topography, where C1 was taken as reference geometry.

	C1	C2	C3	C4	C5
Errors	-0.3 %	-0.1 %	-0.1 %	-2.3 %	-2.3 %

5. Conclusions

In this work, six Ti-6Al-4V cellular specimens produced by SLM were analysed in terms of CAD comparison, thickness distribution and surface morphology. Moreover, simulations of five cylindrical features with different surface topography and known thickness distribution were performed in order to assess the accuracy of CT-based thickness analysis and CAD comparison. It was explained how the CAD comparison analysis can be influenced by structural distortions which can often occur in cellular structures produced by additive manufacturing. Furthermore, the CAD comparison was determined to be less influenced by the surface topography than the thickness analysis. In particular, the thickness analysis was found to be sensitive to the surface quality and the search angle. The search angle was optimized by evaluations performed on the simulated cylindrical features and the thickness analysis of SLM specimens was then improved.

Acknowledgements

The authors would like to thank Mr. Andrea Benatti (Univ. Trento) for the Matlab routine. This work has received funding from University of Padova, projects Nr. CPDA151522/15 and BIRD167853/16.

References

[1] Levy G N et al 2003 Rapid manufacturing and rapid tooling with layer manufacturing (LM) technologies, State of the art and future perspectives *CIRP Annals Man. Tech.* **52(2)** 589-609

[2] Yan C et al 2012 Evaluations of cellular lattice structures manufactured using selective laser melting *International Journal of Machine Tools & Manufacture.* **62** 32-38

[3] Beyer C and Figueroa D 2016 Design and analysis of lattice structures for additive manufacturing *Journal of Manufacturing Science and Engineering.* **138** 121014

[4] Arabnejad S et al 2016 High strength porous biomaterials for bone replacement: A strategy to assess the interplay between cell morphology, mechanical properties, bone ingrowth and manufacturing constraints *Acta Biomaterialia* **30** 345-356

[5] Van Bael S et al 2011 Micro-CT-based improvement of geometrical and mechanical controllability of selective laser melted Ti6Al4V porous structures *Mat Sci Eng A.* **528** 7423-7431

[6] Wits W W et al 2016 Porosity testing methods for the quality assessment of selective laser melted parts *CIRP Annals Man. Tech*. **65(1)** 201-204. doi: 10.1016/j.cirp.2016.04.054

[7] Thompson A et al 2017 Topography of selectively laser melted surfaces: a comparison of different measurement methods *CIRP Annals Man. Tech*. **66** 543-546

[8] Kerckhofs G et al 2008 Validation of x-ray microfocus computed tomography as an imaging tool for porous structures *Review of Scientific Instruments.* **79** 013711

[9] Martz H E et al 2014 CT to evaluate of distortions in stainless-steel AM structures *Proc. of ASPE Spring Topical Meeting* **57**

[10] Townsend A et al 2017 Areal Surface Texture Data Extraction from X-ray Computed Tomography Reconstructions of Metal Additively Manufactured Parts *Precision Engineering*. **48** 254-264

[11] Carmignato S et al 2017 Influence of surface roughness on computed tomography dimensional measurements *CIRP Annals Man. Tech*. **66**, doi:10.1016/j.cirp.2017.04.067

[12] ISO 25178-2:2012 Geometrical Product Specifications (GPS)—Surface Texture: Areal—Part 2: Terms, Definitions and Surface Texture Parameters.